Submission code: 0K6RN59XKD

See this and other abstracts on our website: https://home.sbgf.org.br/Pages/resumos.php

Seismic source parameters of the Itajobi–SP earthquake of April 16, 2025

Nicholas Rainier Bento Imana (UnB), Lucas Vieira Barros (UnB), Letícia Guedes Assunção (UnB)

Seismic source parameters of the Itajobi–SP earthquake of April 16, 2025

Abstract

Brune's source model and envelop waveform inversion techniques were used to determine the seismic source parameters of the 3.4 mR Itajobi earthquake of April 16, 2025. They were determined from an analysis of digital seismograms recorded in six Brazilian Seismographic Network (RSBR) regional stations with distances ranging from 50 to 300 km. A reverse fault with a radius of 200 m, driven by compressional stress of NE-SW orientation with a seismic moment magnitude of 3.6 mW, was identified as the seismogenic source.

Introduction

On April 16, 2025, at 07:14:43.73 (04:14 AM Brasília time), a magnitude 3.4 mR earthquake occurred in Itajobi, north-central São Paulo State, detected by 28 Brazilian Seismographic Network (RSBR) stations. The initial location using SeisComp3 and the IASPEI91 velocity model (Kennett & Engdahl, 1991) was: latitude -21.287, longitude -49.506, depth 3.0 km, with an azimuthal gap of 65°. Relocation with Hypocenter software (Lienert et al., 1986) and the NewBr regional model (Assumpção et al., 2014) refined the coordinates to latitude -21.345, longitude -48.988, depth 1 km, with an azimuthal gap of 83° and RMS residual of 0.5 s.

Seismic source parameters were determined through spectral analysis (for scalar seismic moment, moment magnitude, corner frequency, and stress drop) and envelope waveform inversion (for moment tensor). Both methods yielded consistent moment magnitudes. The focal mechanism indicates reverse faulting, likely striking NW-SE, with P and T axes-oriented NE-SW and vertically, respectively.

The source characterization addressed both physical dimensions and kinematic movement, as well as fault parameters such as azimuth, force orientations, dip, slip direction, seismic moment, and magnitude.

This study aims to relocate the Itajobi earthquake using a velocity model representative of local geological structures and to determine its seismic source parameters through spectral and envelope waveform inversion, based on data from the six nearest RSBR stations (Fig. 2a).

Method

The parameters that define a finite-dimensional seismic focus that are easiest to obtain are the scalar seismic moment (Mo), the length (L) or radius (r) of the fault, and the stress drop ($\Delta\sigma$). The simplest method of obtaining these parameters is based on the characteristics of the amplitude spectrum of the ground displacement or the Fourier transform modulus of the seismograms generated by earthquakes. Brune (1970) and Aki (1967) showed that the ground motion spectrum can be divided into two parts: one for low frequencies, which is approximately flat up to a certain frequency value, and another from a frequency f_0 (corner frequency) after which the spectrum drops proportionally with f^{-2} (Aki, 1967). The constant value of the spectrum is proportional to the seismic moment (M0) (Kanamori, 1977).

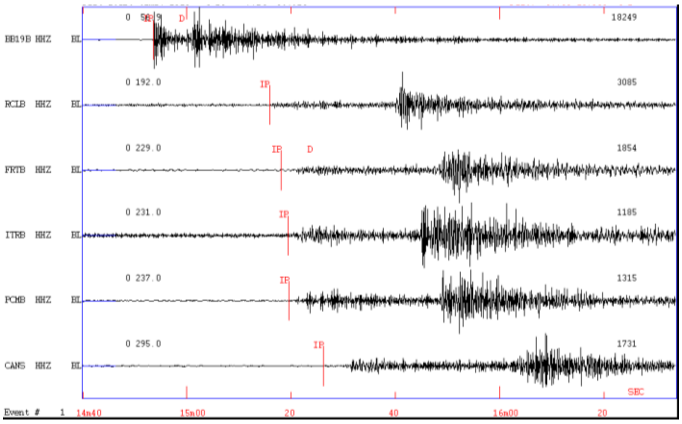

Fig. 1 *– Seismograms of the Itajobi – SP event, on April 16, 2025, vertical components at 6 RSBR stations, used in spectral analysis and waveform envelope inversion.*

Seismic source parameters by spectral analysis

The scalar seismic moment (M_0) quantifies the size of a shear seismic source and is defined by:

$$M_0 = \mu d A \qquad (1)$$

Where μ is the shear modulus, d is the average slip, and A is the rupture area (Kanamori, 1977). For earthquakes without visible surface rupture, Brune's (1970) model allows M_0 to be estimated from the low-frequency level of the displacement spectrum:

$$M_0 = \frac{4\pi r \rho {V^3}_{p/s}\ \Omega_0}{R\theta\phi} \qquad (2)$$

Where r is hypocentral distance, ρ is rock density, V is wave velocity, Rθϕ is the radiation pattern correction, and Ω_0 is the low-frequency spectral amplitude, corrected for instrumental and propagation effects.

The source radius (a) is calculated as:

$$a = \frac{0{,}35v}{f0} \qquad (3)$$

The stress drop in bars (1 bar = 10^6 dynes/ cm^2) was calculated as:

$$\Delta\sigma = \frac{7}{16} M_0 \frac{1}{a^3} * \ 10^{-14} \qquad (4)$$

The original formula assumes that the moment is in dyne-cm and the radius is in cm. The conversion factor 10^{-14} is required for conversion to MKS units. The seismic moment magnitude (Mw) was calculated using the following relation

$$M_W = \frac{2}{3} log M_0 \ - 6{,}06 \qquad (5)$$

Seismic source parameters by envelope waveform inversion

Envelope waveform inversion for the Moment Tensor, proposed by Zahradník and Sokos (2018), is an alternative to standard full waveform inversion, particularly in the case of poor velocity models. This method assumes a 100% double-couple (DC) source and encodes focal mechanism information through variations in envelope shapes and amplitudes among seismogram components. Envelopes of bandpass-filtered waveform displacement are computed, and pure-shear focal mechanisms are grid searched across strike/dip/rake angles. The comparison between real and synthetic envelope shapes is done using L2-norm differences, adjusted by a time shift for optimal cross-correlation, and results are confirmed with available P phase polarities, at least one, but more polarities result in a better solution (Zahradník and Sokos, 2018).

Results

Figures 2 and 3 show the results of the two techniques employed.

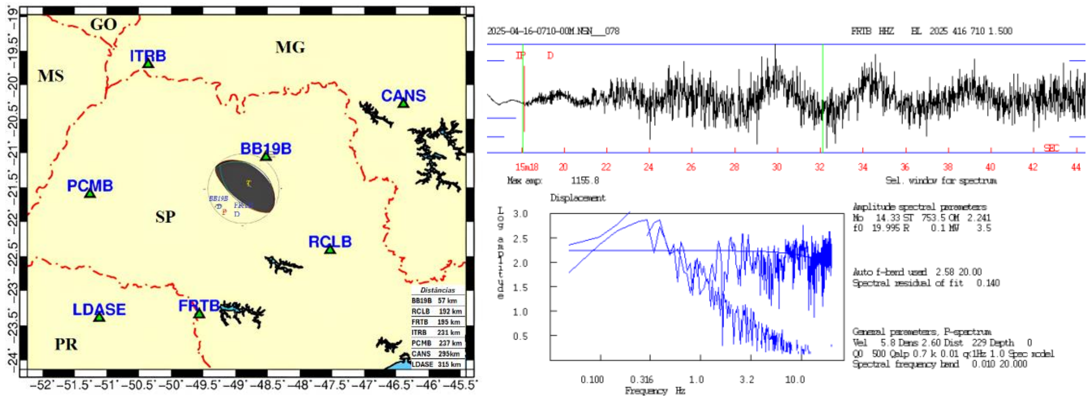

Fig.2 -a) Location of the stations used in the spectral analysis and waveform envelope inversion. The LDASE station, the most distant, was not used. b) Ground displacement spectrum at the FRTB station. The lower trace in displacement refers to the noise level before the arrival time of the P wave.

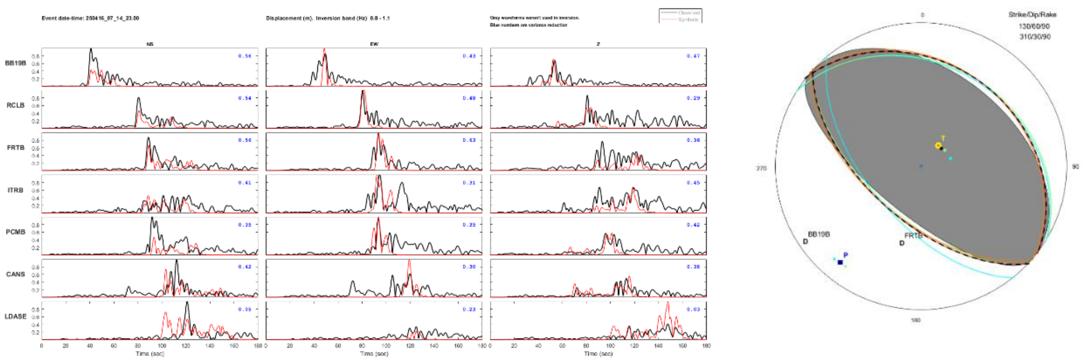

Fig. 3 – a) Waveform envelope correlation at six RSBR stations in the 0.8 to 1.1 Hz band. The last station, LDASE, the most distant, was not used. The red lines represent the synthetic data, and the black ones are the observed data. b) Focal mechanism solution, reverse fault with strike/dip/rake equal to 130º/60º/90º. The polarities at BB19B and FRTB stations are concordant with the focal mechanism solution.

Discussion and conclusions

As is shown in Fig. 2 b), the spectral amplitudes decay rapidly with frequency. Thus, the corner frequency (f_0) marks a critical position in the spectrum related to the source size. According to Brune (1970) and Madariaga (1976), who assumed a circular source model, the corner frequency of the P- or S-wave spectrum is fo p/s = cm Vp/s/πr, while for Haskell (1964), who assumed a rectangular fault, fo p/s = cm Vp,s / (L x W)1/2, where L is the length and W the width of the fault. The cm values are model-dependent constants.

References

Assumpção, M; Urdita, J.; and Barbosa, J.R. (2010). An improved velocity model for regional epicentre determination in Brazil. IV Symposium Brasileiro da SBGf, Brasilia.

Barros, L.V. (2004). Parêmetros de fonte do sismo de P. dos Gaúchos/MT, de 10/03/1998, I Simp SBGf.

Aki, K. (1967). Scaling law of seismic spectrum. J. Geophys. Res., 72, 4, 1217-1231. AKI, K. & P.G. RICHARDS (1980). Quantitative Seismology. Theory and methods. Vol. 1. W.H. Freeman and Company, San Francisco, ISBN 0 7167-1058-7, 557 pp.

Borman, P. (2002) - New manual of Seismological Observatory Practice (NMSOP) V. 1 BRUNE, J. N. (1970) - Tectonic stress and the spectra of seismic shear waves from earthquakes. Geophys. Res. 75, 4997-5009.

Haskell, N. A. (1964). Total energy and energy spectral density of elastic wave radiation from propagating faults. Bull. Seism. Soc. Am. 54, 1811-1841.

Kanamori, H. (1977) - The energy release in great earthquakes: Journal of Geophysical Research, v. 82, p. 2981-2987.

Kennett, B. L. N., & Engdahl, E. R. (1991). Travel times for global earthquake location and phase identification. Geophysical Journal International, 105(2), 429–465.

Lienert, B. R. E., Berg, E., & Frazer, L. N. (1986). Hypocenter: An earthquake location method using centered, scaled, and adaptively damped least squares. Bulletin of the Seismological Society of America, 76(3), 771–783.

Madariaga, R. (1976). Dynamics of an expanding circular fault. Bul. Seism. Soc. Am 66, 639-666.

Ottemöller, L., Voss, P.H. and Havskov J. (2021). SEISAN Earthquake Analysis Software for Windows, Solaris, Linux, MacOSX, Version 12.0. 607 pp.m. University of Bergen. ISBN 978-82-8088-501-2, URL http://seisan.info.

Zahradník, J., and E. Sokos, 2018, Fitting Waveform Envelopes to Derive Focal Mechanisms of Moderate Earthquakes, Seismological Research Letters, 89, no. 3, 1137–1145, doi: 10.1785/0220170161